INL/CON-23-73248-Revision-0

Implementation of a High-Fidelity Interface Resolving Method in Nek5000

November 2023

Donna Post Guillen, Nadish Saini, Dillon Shaver

Changing the World's Energy Future

INL is a U.S. Department of Energy National Laboratory operated by Battelle Energy Alliance, LLC

INL/CON-23-73248-Revision-0

Implementation of a High-Fidelity Interface Resolving Method in Nek5000

Donna Post Guillen, Nadish Saini, Dillon Shaver

November 2023

Idaho National Laboratory
Idaho Falls, Idaho 83415

http://www.inl.gov

Prepared for the
U.S. Department of Energy
Under DOE Idaho Operations Office
Contract DE-AC07-05ID14517

Implementation of a High-Fidelity Interface Resolving Method in Nek5000

Donna P. Guillen[1], Nadish Saini[2], Dillon R. Shaver[2]

[1]*Idaho National Laboratory, 1955 N. Freemont Ave., Idaho Falls, ID 83415, donna.guillen@inl.gov*
[2]*Argonne National Laboratory, 9700 S Cass Ave, Lemont, IL 60439, dshaver@anl.gov, nsaini@anl.gov*

INTRODUCTION

The development and utilization of computational fluid dynamics (CFD) models for large, high-temperature electric melters in the Waste Treatment and Immobilization Plant (WTP) in eastern Washington State have proven to be valuable for various purposes. These models allow for a better understanding of the physio-chemical processes occurring within the melter vessels and can contribute to improving operational efficiency, throughput, and addressing operational issues related to vitrification.

The CFD models employed for these melter vessels incorporate multiphase fluid flow and heat transfer simulations in different regions, including the plenum, cold cap, and molten glass regions. As the tank waste and glass formers are introduced into the melter, a reacting batch layer known as the cold cap forms on top of the molten glass. To enhance the melt rate, forced convection bubblers located at the bottom of the melters generate convection currents that help homogenize the molten glass and provide heat to the cold cap. As the bubbles rise through the highly viscous glass, they adopt a spherical-cap shape [1]. Meanwhile, the conversion of the batch to glass generates significant amounts of gases (such as water vapor, carbon dioxide, sulfur dioxide, and NOx) due to thermal decomposition [2]. These gases become trapped between the cold cap and molten glass, forming a foam layer [3].

For modeling multiphase flow in CFD and heat transfer simulations of waste glass melters at different scales, efforts are underway to augment the capabilities of the Nek5000 [4] and NekRS [5] open-source codes [6]. Nek5000/NekRS is a scalable and efficient spectral element code that has been successfully applied to a wide range of fluid dynamics problems. By leveraging the Nek5000/NekRS software, it becomes possible to model the melter systems more affordably and with lower computational requirements compared to currently utilized commercial CFD software.

The specific objectives of this ongoing effort include:

1. Implementation of a level set method in Nek5000/NekRS: The level set method is a numerical technique commonly employed in CFD simulations to track and represent the interface between different phases or materials accurately. By incorporating this method into Nek5000/NekRS, the ability to simulate multiphase flows in waste glass melters at a high level of fidelity can be achieved.
2. Demonstration of capability for air bubbling through molten glass: As part of the development process, a specific case of air bubbling through molten glass will be simulated using the augmented Nek5000/NekRS code. This demonstration aims to showcase the ability of the software to accurately capture and analyze the complex phenomena involved in the multiphase flow within waste glass melters.

By achieving these objectives, the improved Nek5000/NekRS code will offer a powerful computational tool for simulating and analyzing waste glass melter systems, enabling better understanding, optimization, and troubleshooting of these vitrification processes. The ability to accurately model and simulate multiphase flows has broad relevance across many industries and scientific domains, and the improved functionality can contribute to advancements in various fields beyond waste glass melter simulations.

METHODOLOGY

Theory

The level set method has been demonstrated to be a robust method for simulating flows of two immiscible Newtonian fluids on numerical grids and resolving multiphase interfaces. Previous approaches comparing the results of a finite volume approach to a level set technique for rising spherical-cap bubbles have produced similar results [7].

Within the level set method, immiscible liquids are identified in the domain using a continuous field function which can be a signed distance function [7] or a diffuse step function [8]. In numerical computations, to preclude a sharp discontinuity, the properties between the fluids are smeared across a finite length which has a length scale equivalent to the mesh resolution. The level set field is transported as a passive scalar, assuming there is no-phase change, advecting the interface based on the local flow field. Owing to high gradients across the interface, transport of the level set field invariably results in spurious oscillations. In addition, a non-linear re-distancing equation is imperative to restore the signed distance property or to maintain the sharpness of the step function, depending on the type of level set field function employed, to maintain accurate curvature of the interface needed for the application of surface tension force. Thus, stabilization of the (linear) level set advection equation and (non-linear) re-distancing equation is imperative for successfully resolving the interface in two-phase simulations.

To meet this objective, two stabilizing mechanisms were implemented in Nek5000, specifically tailored for the continuous Galerkin spectral element method, and are tested in this work for linear scalar advection problems with a sharp discontinuity.

The first method was introduced by Lu et al. [9] and it augments a linear hyperbolic advection problem with a non-linear artificial diffusion term,

$$\frac{\partial \phi}{\partial t} + \vec{u} \cdot \nabla \phi = \nabla \cdot (\nu_a(\vec{x}, t) \nabla \phi); \vec{x} \in \Omega, t > 0 \tag{1}$$

where ϕ is the transported field with irregularity in the initial condition, $\phi_0(\vec{x})$, $\vec{u}$ is assumed to be divergence free velocity field and the right hand side term is the added artificial diffusion term with $\nu_a(\vec{x}, t)$ being the non-linear diffusion coefficient. Lu et al. presented several methods for conceptualizing the artificial diffusion term which can be encapsulated by

$$\nu_a(\vec{x}) = \min(\gamma h |\vec{u}|, c_E h^2 r_E(\phi)) \tag{2}$$

where γ and c_E are order-unity tunable constants, h is a characteristic length scale and corresponds to local grid spacing, and r_E is an error indicator which provides a measure of local irregularity of the solution. r_E can be constructed in several different ways, as elaborated in Lu et al. [9]. Here, we consider the residual based on high pass filtered solution,

$$r_E(\phi) = f(HPF(\phi^{n-1})) \tag{3}$$

where the high pass filter (HPF) is applied to the solution at the previous time step. Since irregularity in the local solution will manifest as significant magnitude of the high wavenumbers, the above construction provides a measure of the irregularity of the solution. Note that for locally smooth solution $||HPF(\phi)||$ is exponentially small. Further details on the artificial viscosity method (AVM) are omitted here, for brevity.

The second approach we consider is the spectrally vanishing viscosity (SVV) method, wherein the artificial diffusion term is constructed using a convolutional tensor, written as,

$$\frac{\partial \phi}{\partial t} + \vec{u} \cdot \nabla \phi = \mu \nabla \cdot \boldsymbol{Q} \cdot \nabla \phi; \vec{x} \in \Omega, t > 0 \tag{4}$$

where $\boldsymbol{Q}$ is the convolutional tensor applied to the derivatives in the physical domain, Ω. We, however, do not explicitly define the convolution in the physical space. Instead, the convolution is applied orthogonally in the computational space, $\widehat{\Omega}(\vec{r})$, and geometric factors are then applied to map the convoluted derivatives onto the physical space. To illustrate, we proceed to write the weak form of the diffusion term,

$$\int_\Omega \nabla v \cdot \boldsymbol{Q} \cdot \nabla \phi \, d\Omega \equiv \int_\Omega \frac{\partial v}{\partial x_i} Q_{ij} \frac{\partial \phi}{\partial x_j} d\Omega \, ; \forall v(\vec{x}) \in V \tag{5}$$

where $V = H^1(\Omega)$ is the space of square integral functions in Ω. Employing the chain rule for evaluating the derivatives, the integral is written in the computational space as,

$$\begin{aligned} &\int_{\widehat{\Omega}} \left(\frac{\partial v}{\partial r_l}\frac{\partial r_l}{\partial x_i}\right) Q_{ij} \left(\frac{\partial r_m}{\partial x_j}\frac{\partial \phi}{\partial r_m}\right) J_e d\Omega \\ &\equiv \int_{\widehat{\Omega}} \left[\hat{Q} * \frac{\partial v}{\partial r}\right]_l \frac{\partial r_l}{\partial x_k}\frac{\partial r_m}{\partial x_k} \left[\hat{Q} * \frac{\partial \phi}{\partial r}\right]_m J_e d\Omega \end{aligned} \tag{6}$$

where $\hat{Q} * (\cdot)$ denotes the convolutional operator applied to the derivatives in computational space, $\widehat{\Omega}(\vec{r})$. In matrix form the right hand side representation of the above integral is (written for simplicity in 2D),

$$\int_{\widehat{\Omega}} \begin{bmatrix} \frac{\partial v}{\partial r_1} \\ \frac{\partial v}{\partial r_2} \end{bmatrix} \begin{bmatrix} \hat{Q}_1 & 0 \\ 0 & \hat{Q}_2 \end{bmatrix} \begin{bmatrix} \hat{G}_{11} & \hat{G}_{12} \\ \hat{G}_{21} & \hat{G}_{22} \end{bmatrix} \begin{bmatrix} \hat{Q}_1 & 0 \\ 0 & \hat{Q}_2 \end{bmatrix} \begin{bmatrix} \frac{\partial \phi}{\partial r_1} \\ \frac{\partial \phi}{\partial r_2} \end{bmatrix} J_e d\Omega \tag{7}$$

where $\hat{G}_{lm} = \frac{\partial r_l}{\partial x_k}\frac{\partial r_m}{\partial x_k}$ are the geometric factors that map the derivatives onto physical space, J_e is the mapping Jacobian and $\hat{Q}_i$ is the convolution kernel applied to the derivative in i direction. Note that the overall convolution matrix is diagonal. Thus, a unique kernel can be applied to each directional derivative independently. Subsequently, expansion of spectral element basis and application of numerical quadrature at the GLL points (Gauss-Lobatto-Legendre) leads to the following discrete form,

$$\underline{v}^{e^T} \boldsymbol{D}^T \tilde{\boldsymbol{Q}}^T \boldsymbol{G} \tilde{\boldsymbol{Q}} \boldsymbol{D} \underline{u}^e = \underline{v}^{e^T} \boldsymbol{S}^e_{vv} \underline{u}^e \tag{8}$$

v_e and u_e correspond to the coefficients of polynomial expansion for an element, $\boldsymbol{G}$ is the discrete matrix comprising geometric factors and quadrature weights and $\boldsymbol{D} = [D_1 \quad D_2]^T$ is the discrete derivative matrix (see Deville et al. [10] for further details). $\tilde{\boldsymbol{Q}}$ consists of diagonal entries with discrete convolution kernel which are constructed in the wavenumber space using modal Legendre basis,

$$\tilde{Q}_{ii} = \tilde{B} \tilde{Q}_i \tilde{B}^{-1} \tag{9}$$

where $\tilde{B} = \hat{B} \otimes \hat{B}$; $\hat{B}$ being the 1D Legendre basis (Vandermonde) matrix operator and $\tilde{Q}_i$ is a HPF matrix, written for each direction using tensor product applied to 1D filter matrix $\hat{Q}$,

$$\tilde{Q}_1 = I \otimes \hat{Q}; \tilde{Q}_2 = \hat{Q} \otimes I \tag{10}$$

The diagonal entries in the 1D filter matrix correspond to wavenumber index. In this work we employ the power kernel, as defined by Moura et al. [11],

$$\hat{Q}_{ij} = \begin{Bmatrix} \left(\frac{i-1}{N}\right)^{\frac{N}{4}} & i = j \\ 0 & i \neq j \end{Bmatrix} \quad (11)$$

where N is the polynomial order of approximation. In Eq. (4), μ is a local viscosity scaling coefficient which can be linear or non-linear, defined as,

$$\mu = \frac{c_0}{N} c_{nl} |\vec{u}| h \quad (12)$$

c_0 is an order-unity constant and c_{nl} is a dimensionless scaling parameter which is equal to unity for linear construction of SVV and designed to scale with the magnitude of regularity of local solution, similar conceptually to the shock detectors by Persson et al. [12]. Details of the construction of c_{nl} are omitted here for brevity.

RESULTS

Linear Advection of 1D Discontinuity

Linear advection of initial discontinuous solution are highly suited problems for testing shock capturing methods since the exact solution at any time instance is known and the discontinuities are not self-steepening which provides a measure of the magnitude of diffusivity of the method under consideration. Fig. 1 shows the initial solution considered for demonstration with a triangular, square, and parabolic discontinuities defined on a 1D periodic domain. 50 spectral elements of polynomial order 9 are used for the mesh. Fig. 1 also shows the solution from the AVM, linear SVV and non-linear SVV(SVV-NL) at t=1 (one periodic rotation). While the linear SVV shows some significant overshoots/undershoots near the square discontinuity, AVM and non-linear SVV show comparable overall profile. All methods capture the triangular and parabolic profile which have continuous initial profile, however, feature sharp gradients.

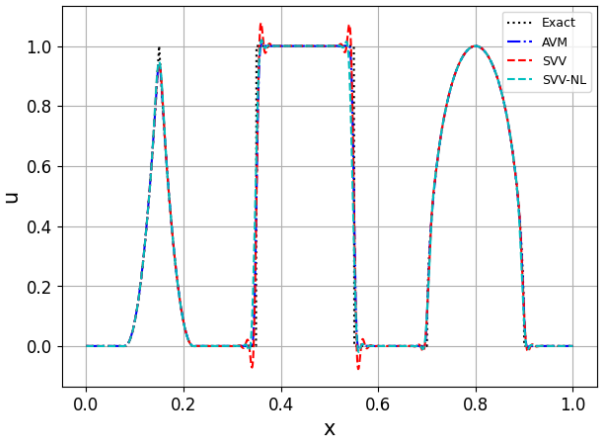

Fig. 1. Comparison of AVM and linear and non-linear SVV at t=1.

Fig. 2 demonstrates the behavior of AVM and SVV on long time integration of the solution; profiles shown at t=10 (10 rotations). All methods show only slightly more smearing near the square shock, as compared to profile at t=1. Thus, the methods show excellent transport properties for stabilized linear hyperbolic problems.

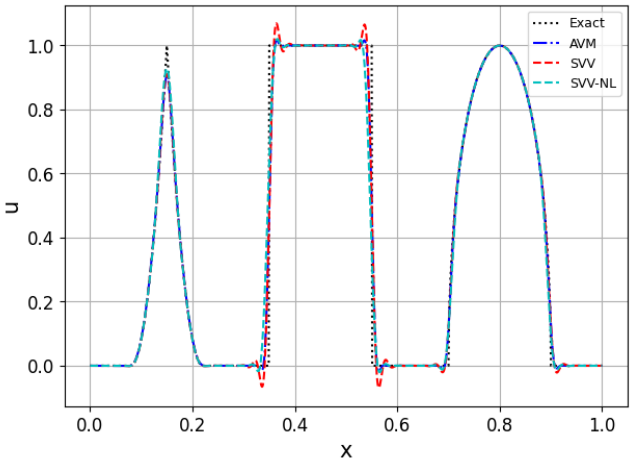

Fig. 2. Comparison of AVM and linear and non-linear SVV at t=10.

Zalesak Problem

The Zalesak pole problem, which comprises a partially slotted pole in a 2D domain with divergence free rotational velocity field, has been extensively used in literature as a rigorous test case for stabilizing scheme, especially to test the methods for application to level set problems [13]. The velocity field for the problem is defined as,

$$u_x = \pi(0.5 - y) \quad (13)$$
$$u_u = \pi(x - 0.5)$$

while the initial solution is given as,

$$\phi_0 = \begin{cases} 1 & r \leq 0 \;\&\; (|x| < 0.025 \;\&\; y < 0.85) \\ 0 & otherwise \end{cases} \quad (14)$$

where $r = \sqrt{(x-0.5)^2 + (y-0.75)^2} - 0.15$. The domain is periodic on all ends and is defined by the extent $\Omega = [0,1]$. The mesh consists of 50X50 elements of order 9.

Fig. 3 shows the profile across the horizontal line at $y = 0.75$ obtained with various artificial viscosity methods. Similar to the 1D case, the linear SVV method shows persistent overshoots and undershoots near the vicinity of the discontinuity. While the non-linear SVV method ameliorates these features, AVM gives the best performance for this case. Nevertheless, all methods provide robust advection of the initial discontinuity and are effective in capturing the sharp gradients.

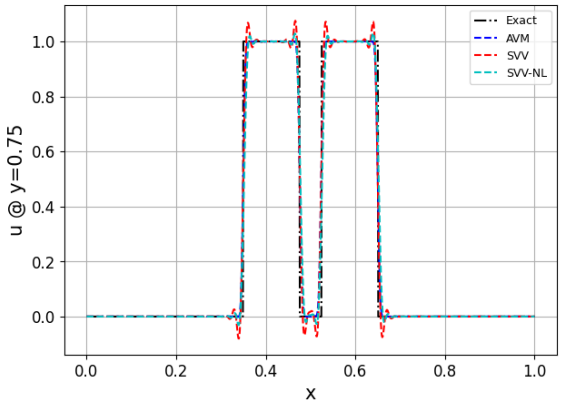

Fig. 3. Comparison of AVM and linear and non-linear SVV profile at y=0.75 after one rotation.

CONCLUSIONS AND FUTURE WORK

The ability to model multiphase flows using the level set method in Nek5000/NekRS codes will enable simulation of melter systems with high fidelity. The spectral element method (SEM), which forms the basis of these CFD codes, exhibits negligible numerical diffusion which is highly favorable for tracking the interface of multiphase fluid systems. However, stabilization of transport equations is imperative since the level set field invariably features strong gradients, especially near the interface, which can lead to spurious oscillations. Two stabilization methods, developed for the specific context of SEM are discussed herein and applied to 1D and 2D linear advection problems with initial discontinuous solution. Future work will include detailed analysis of the stabilization methods, with parameter tuning to provide robust stabilization with minimal diffusion added to the regular regions of the domain. Subsequently, the stabilization method will be adopted for interface capturing simulation in Nek5000/NekRS.

ACKNOWLEDGEMENTS

This work was supported by Dr. Albert Kruger of the United States Department of Energy's (DOE's) WTP Project at the Office of River Protection. This study was authored by Battelle Energy Alliance, LLC under Contract No. DE-AC07-05ID14517 and made use of the resources of the High Performance Computing Center at Idaho National Laboratory, which is supported by the Office of Nuclear Energy of the U.S. DOE and the Nuclear Science User Facilities. The manuscript has been created in part by UChicago Argonne, LLC, Operator of Argonne National Laboratory ("Argonne"), a U.S. DOE Office of Science laboratory operated under Contract No. DE-AC02-06CH11357. The U.S. Government retains for itself, and others acting on its behalf, a paid-up, nonexclusive, irrevocable worldwide license in said article to reproduce, prepare derivative works, distribute copies to the public, and perform publicly and display publicly, by or on behalf of the Government.

REFERENCES

1. D.P. GUILLEN, "Bubbling Behavior in a Waste Glass Melter", *WIT Transactions on Engineering Sciences*, **105**, 75-85, WIT Press, (2016). https://doi.org/10.2495/AFM160071
2. P. FERKL, P. HRMA, A. ABBOUD, D.P. GUILLEN, M. VERNEROVA, J. KLOUZEK, M. HALL, A.A. KRUGER, R. POKORNÝ, "Conversion degree and heat transfer in the cold cap and their effect on glass production rate in an electric melter," *International Journal of Applied Glass Science*, (2022). https://doi.org/10.1111/ijag.16615
3. A.W. ABBOUD, D.P. GUILLEN, P. HRMA, A.A. KRUGER, J. KLOUZEK, R. POKORNY, Heat Transfer from Glass Melt to Cold Cap: Computational Fluid Dynamics Study of Cavities Beneath Cold Cap, *International Journal of Glass Science*, 12(2), 233-244, (2021). https://doi.org/10.1111/ijag.15863
4. NEK5000 Version 19.0. Release date Dec 28, 2019. Argonne National Laboratory, Illinois. Available: https://nek5000.mcs.anl.gov.
5. NEKRS Version 23.0. Release date Mar 31, 2023. Argonne National Laboratory, Illinois. Available : https://github.com/Nek5000/nekRS
6. A.W. ABBOUD, D.P. GUILLEN, "Simulating Waste Glass Melters with the Spectral Element Method," ANS Transactions, **128** (2023).
7. D.P. GUILLEN, J. CAMBARERI, A.W. ABBOUD, I.A. BOLOTNOV, "Numerical Comparison of Bubbling in a Waste Glass Melter," *Annals of Nuclear Energy,* **113**, 380–392, (2018). https://doi.org/10.1016/j.anucene.2017.11.044
8. M. OWKES, O. DESJARDINS. "A Discontinuous Galerkin Conservative Level Set Scheme for Interface Capturing in Multiphase Flows," *Journal of Computational Physics,* **249**, 275-302 (2013).
9. L. LU, N. MURTAZO, P. FISCHER. "Nonlinear artificial viscosity for spectral element methods." *Comptes Rendus Mathematique* **357.7,** 646-654 (2019).
10. M.O. DEVILLE, P. F. FISCHER, E.H. MUND. "High-Order Methods for Incompressible Fluid Flow," Vol. 9. *Cambridge University Press* (2002).
11. R.C. MOURA, S.J. SHERWIN, J. PEIRÓ. "Eigensolution Analysis of Spectral/Hp Continuous Galerkin Approximations to Advection–Diffusion Problems: Insights into Spectral Vanishing Viscosity," *Journal of Computational Physics* **307** 401-422, (2016).
12. P.-O. PERSSON, J. PERAIRE. "Sub-Cell Shock Capturing for Discontinuous Galerkin Methods," 44th AIAA Aerospace Sciences Meeting and Exhibit (2006).
13. S.T. ZALESAK, "Fully Multidimensional Flux-Corrected Transport Algorithms for Fluids," *Journal of Computational Physics* **31.3**, 335-362 (1979).